Microstructure and spectroscopy studies on cubic boron nitride synthesized under high-pressure conditions

Microstructure and spectroscopy studies on cubic boron nitride synthesized under high-pressure conditions

L C Nistor[1]**, S V Nistor**[1]**, G Dinca**[2]**, P Georgeoni**[2]**, J Van Landuyt**[3]**, C Manfredotti**[4] **and E Vittone**[4]

[1] National Institute for Materials Physics, Bucharest, Romania
[2] Dacia Synthetic Diamonds Factory, Bucharest, Romania
[3] University of Antwerpen—RUCA, EMAT, Antwerpen, Belgium
[4] Experimental Physics Department, University of Turin, Turin, Italy

E-mail: r&d_rdacia@ines.ro (G Dinca)

Abstract
High-resolution electron microscopy (HREM) studies of the microstructure and specific defects in hexagonal boron nitride (h-BN) precursors and cubic boron nitride (c-BN) crystals made under high-pressure high-temperature conditions revealed the presence of half-nanotubes at the edges of the h-BN particles. Their sp^3 bonding tendency could strongly influence the nucleation rates of c-BN. The atomic resolution at extended dislocations was insufficient to allow us to determine the stacking fault energy in the c-BN crystals. Its mean value of 191 ± 15 mJ m^{-2} is of the same order of magnitude as that of diamond. High-frequency (94 GHz) electron paramagnetic resonance studies on c-BN single crystals have produced new data on the D1 centres associated with the boron species. Ion-beam-induced luminescence measurements have indicated that c-BN is a very interesting luminescent material, which is characterized by four luminescence bands and exhibits a better resistance to ionizing radiation than CVD diamond.

1. Introduction

Cubic boron nitride (c-BN), the second hardest material known, after diamond, exhibits a high thermal conductivity and excellent ability to be n and p doped, which makes it a potential candidate for use in microelectronic devices [1]. According to recent studies, c-BN exhibits a better resistance to radiation damage than diamond [11], which suggests potential applications in extreme radiation environments. However, for the time being, the electronic applications of c-BN are restricted by the limited size of the high-pressure (HP) samples and imperfect structure of the low-pressure (LP) materials.
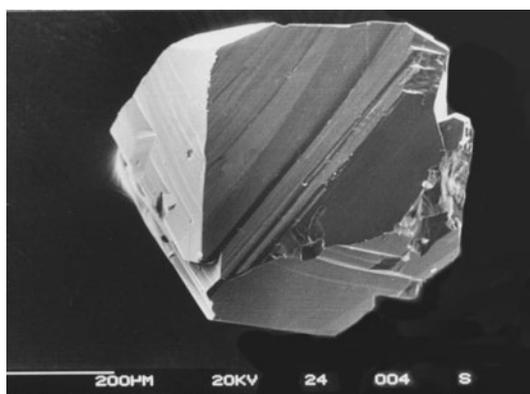
Figure 1. An individual c-BN crystal grown on a seed.

In this paper we present relevant data concerning the importance of the h-BN microstructure for c-BN growth at HP, the microstructure and specific defect species in h-BN and c-BN crystals and recent measurements on ionoluminescence characteristics of c-BN crystals made at HP.

2. c-BN synthesis

The synthesis experiments were carried out in a straight-bore belt-type HP apparatus. As flux precursors we used nitrides and boronitrides of Li, Ca and Mg mixed with fluorides and chlorides [2, 3].

The starting raw materials were well-crystallized h-BN powders with a very low content of boron oxide and a graphitization index (GI) between 1.56 and 4.97.

Cubic BN single crystals of sizes over 40 mesh (minimum 420 μm) were obtained by a controlled seeding technique under high-pressure–high-temperature (HPHT) conditions. The seeds were c-BN grains of around 200 μm in size. Their initial concentration was estimated at about 600 particles cm^{-3}. The resulting c-BN crystals exhibit tetrahedral shapes and growth steps (figure 1). Also, their colour varies from yellow to dark brown, depending on the nature of the solvent–catalyst and doping species.

Sintered c-BN pellets were prepared by subjecting c-BN micron powders to pressure over 6.0 GPa and temperature around 1600 °C. The sintered bodies were used in the ion luminescence analysis.

3. h-BN precursors

From the study of the influence of the structural characteristics of h-BN precursors on the HPHT c-BN synthesis yields, we noticed that compared with that based on the well-known GI [4], a better assessment can be performed by examining the microscopic features of the h-BN particles [5]. In this study we used h-BN powders with GI between 1.56 and 7.5. GIs were derived from x-ray diffraction data as the ratio between the area under the [(100) + (101)] peaks to the area under the (102) peak. They describe the degree of order in the stacking of the BN layers along the c-axis. Well-crystallized (GI < 7) h-BN powders are usually chosen for c-BN synthesis. As in the case of graphite, the morphology of the h-BN crystallites is
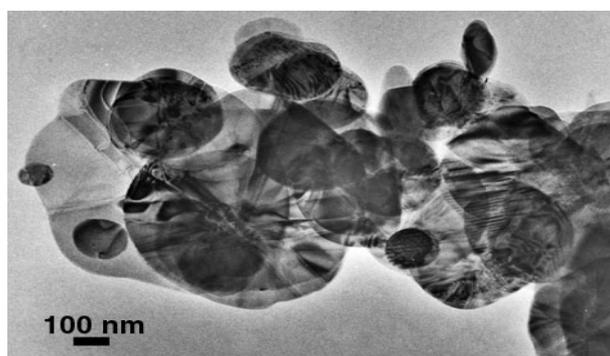
Figure 2. A TEM image of an aggregate of h-BN crystallites viewed along the [0002] zone axis.
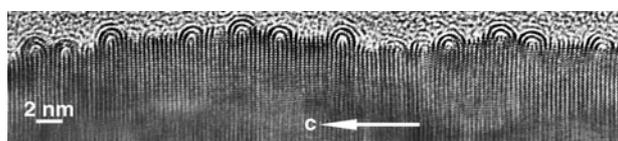

Figure 3. A HREM image along the $[\bar{1}2\bar{1}0]$ zone axis of the edge of a h-BN crystallite showing nanoarches formed during the sample synthesis.

platelet-like or even foil-like (figure 2). There is also a large variation in average crystallite diameter between different h-BN samples.

An average value of the diameter ($\bar{D}$) and thickness ($\bar{t}$) can be statistically determined for each specimen. The ratio $\bar{t}/\bar{D}$ measures the sample morphology. The GI values and the $\bar{t}/\bar{D}$ values are fairly proportional. Differences between the two factors occur when the crystal coherency along the c-direction is broken.

The GI factor depends on both the diameter of the h-BN crystallite and the stacking order of the hexagonal planes. In the $\bar{t}/\bar{D}$ determination, the measured crystal thickness depends on its morphology and is not influenced by the presence of the stacking faults.

More detailed structural information regarding the stacking order of the hexagonal planes can be obtained from the electron diffraction patterns along the $[\bar{1}2\bar{1}0]$ zone axis, which contain all the reflections used for the calculation of the graphitization indices.

Very interesting results were obtained when examining the edge of the h-BN specimens by HREM along the $[\bar{1}2\bar{1}0]$ zone axis. Cylindrical curving of the h-BN graphitic sheets at the crystallite edge can be observed, as shown in figure 3. In this case many of the (0002) planes bend back and join in pairs. The result is the formation of nanoarches (BN half-nanotubes) at the edge of the h-BN crystallites.

The largest nucleation rates for c-BN were observed for the h-BN powders with a large density of nanoarches at their edge. It is thus possible that these nanoarches constitute nucleation centres for c-BN. According to [6], when the graphitic sheet bends, the N–B bond bends too and locally the bonding changes its character from sp^2 to sp^3, like in c-BN. The energy of these highly curved nanostructures should increase due to introduction of strain or lattice defects.
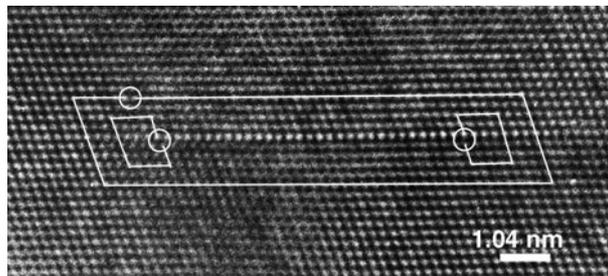
Figure 4. A HREM image of a dissociated 60° dislocation.

4. The c-BN characterization

4.1. Extended defects in c-BN

Diffraction contrast experiments show that the most frequently observed extended defects are dislocations. Dislocations tend to agglomerate, forming dislocation tangles. As in diamond, the dislocation slip system in c-BN is $\langle 110 \rangle \{111\}$, but at dislocation cores the atoms are either B or N. In c-BN crystals the dislocations most frequently observed were of the pure screw type. This is quite natural for a polar crystal. Figure 4 shows a 60° dislocation which is dissociated into a stacking fault bordered by two partial dislocations. Burgers circuits are drawn around the whole dislocation and the partials. Such images were used to calculate the stacking fault energy by measuring the fault length.

The calculation of the stacking fault energy γ is based on the relation for the equilibrium separation between partials [7]. The separation d between partials can be directly measured on HREM images, with a precision limited by the uncertainty in localizing the cores. For the 60° dislocation, $\gamma = 134 \pm 10$ mJ m^{-2}; and for the screw dislocation, $\gamma = 248 \pm 21$ mJ m^{-2}. An average value of 191 ± 15 mJ m^{-2} obtained for several ribbons is smaller than that for diamond, but of the same order of magnitude. For diamond, $\gamma = 209\text{--}279 \pm 41$ mJ m^{-2} [8].

4.2. EPR studies on c-BN

Electron paramagnetic resonance (EPR) spectroscopy is the most powerful technique for identification and characterization of paramagnetic point defects in insulating and semiconducting crystals.

Low-frequency X-band (9.4 GHz) EPR measurements performed on c-BN powders containing dark-brown crystallites revealed the presence of a characteristic composite spectrum, called the D (from dark) spectrum [9]. Such an EPR spectrum could not be observed for any of the samples containing only yellow/amber crystallites.

The deconvolution of the D spectrum recorded at RT unveils a superposition of two clearly Lorentzian lines called D1 and D2, centred at $g1 = 2.0063 \pm 0.0002$ and $g2 = 2.0084 \pm 0.0006$, with linewidth of 3.3 and 17.9 mT, respectively. The presence of both D1 and D2 only for dark-brown c-BN crystals prepared with, and known to contain excess of, boron strongly suggests that boron is directly involved in the formation and microscopic structure of both D centres.

Further studies by means of high-frequency W-band (94 GHz) EPR on brown-to-dark-brown single crystals, at low temperatures, identified the D1 species (figure 5) as consisting mainly of anisotropic paramagnetic centres with electron spin $S = 1/2$, local symmetry along one of the crystal axes and principal g-values $g_{\parallel} = 2.0032 \pm 0.0009$ and $g_{\perp} = 2.0094$ at $T = 10$ K [10].
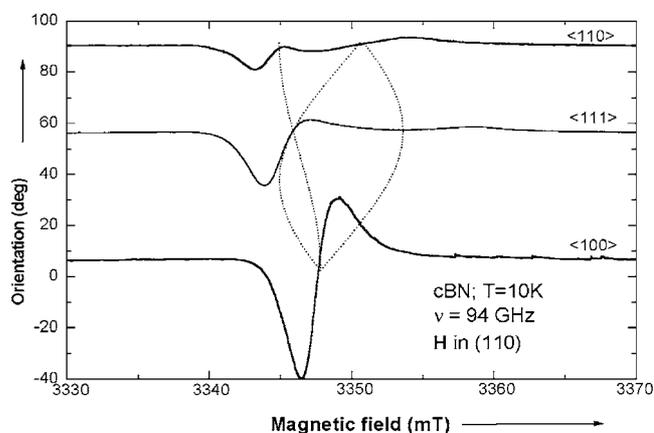
Figure 5. Experimental EPR spectra attributed to the D1 centre in brown–dark-brown c-BN single crystals.

Unfortunately, for the time being, no resolved hyperfine structure due to the magnetic interaction between the unpaired electron and the nuclear spins of the c-BN lattice atoms could be observed for any orientation of the magnetic field in the (110) and (111) crystal planes, down to the lowest attainable temperature (5 K). Finding the proper conditions in which the hyperfine structure becomes observable is essential for establishing a unique structural model of D centres in c-BN.

4.3. IBIL studies on c-BN

The first measurements on the ion luminescence induced in c-BN sintered bodies, by 2 MeV protons, were recently reported [11]. c-BN is mainly characterized by four luminescence bands (table 1). The ion-beam-induced luminescence (IBIL) spectra are very resistant to radiation, even more so than those of diamond.

The intensities of some bands are probably dependent on the main flux impurity content (Mg and Ca).

5. Conclusions

(1) The study of the microscopic features of the h-BN powders revealed, as its prime novel feature, that microstructural modifications of their crystallites, such as highly curved BN nanostructures, can act as nucleation centres for c-BN, influencing the reactivity of the h-BN–c-BN catalytic transformation.

(2) Structural studies by the electron microscopy technique show that the most important extended defects, which are largely controlling the mechanical properties of c-BN, are dislocations. The formation energy of stacking faults in c-BN crystals was determined from the equilibrium distance between two partials. It is of the same order of magnitude as in diamond.

(3) Two paramagnetic centres, D1 and D2, were first identified in c-BN crystals grown with excess of boron. Further EPR experiments will try to identify their hyperfine structure in order to establish a structural model for them.

(4) Recent ionoluminescence measurements on c-BN crystals made at HPHT demonstrate that c-BN is a potential candidate for use in thermoluminescence dosimetry.

Acknowledgment

References

[1] Edgar J H (ed) 1994 *Properties of Group III Nitrides* (Kansas City, KS: Kansas State University Press)
[2] Dinca G *et al* (ed) 1994 *Advances in New Diamond Science and Technology* (Tokyo: MY Press) p 663
[3] Demazeau G 1995 *Diam. Relat. Mater.* **4** 284
[4] Thomas J Jr *et al* 1963 *J. Am. Chem. Soc.* **84** 4619
[5] Nistor L *et al* 2001 *Diam. Relat. Mater.* **10** 1352
[6] Widany J *et al* 1996 *J. Mater. Chem.* **6** 899
[7] Amelinckx S 1979 *Dislocations in Solids* ed F R N Nabarro (Amsterdam: North-Holland)
[8] Nistor L C *et al* 1999 *Diam. Relat. Mater.* **8** 738
[9] Nistor S V *et al* 2000 *Solid State Commun.* **115** 39
[10] Nistor S V *et al* 2001 *Diam. Relat. Mater.* **10** 1408
[11] Manfredotti C *et al* 2001 *Diam. Relat. Mater.* **10** 568